

CHAPTER FIVE

***PHYSICOCHEMICAL AND PHYSICOMECHANICAL CHARACTERIZATION OF
THE OPTIMIZED POLYAMIDE 6,10 MONOLITHIC MATRIX SYSTEMS***

5.1. INTRODUCTION

In summary, the efficiency and suitability of experimental designs in executing scientific experimental plans as well as an optimization tool was established in Chapter Two using the Plackett-Burman template. In order to develop principal and flexible polyamide 6,10 monolithic matrix formulations for further investigations and characterization in Chapters Four and Five respectively, a higher performance Box-Behnken design was employed in Chapter Three.

Based on the remarkable and attractive drug delivery performances exhibited by the newly produced optimized polyamide 6,10, monolithic matrix systems (i.e. the slow, intermediate and controlled release optimized monolithic matrix formulations represented as “SR”, “IR” and “CR” respectively), the current Chapter details their characterization process. These polymeric chemical compounds are characterized in terms of their physicochemical and physicochemical properties, which are especially relevant to their use as drug delivery systems. This typical approach may be useful for the identification and/or quality control of these compounds in the near future as well as other polymers that can be employed in the fabrication of drug delivery systems.

5.1.1. Objectives

This experimental Chapter is directed towards characterizing the optimized polyamide 6,10 monolithic matrices developed in Chapter Three in terms of their physicochemical and physicochemical properties as well as relating this to their use as drug delivery systems. This objective will be achieved using textural profile analysis, melting point determination using differential scanning calorimetry, X-ray powder diffractometry, scanning electron microscopy, Fourier transform infrared spectrophotometry, mass

spectrometry, conductivity testing, swelling and water uptake efficiency, matrix erosion and dissolution analysis.

5.2. EXPERIMENTAL SECTION

5.2.1. Materials

The materials and their respective sources employed in this part can be located in the previous experimental Chapters.

5.2.2. Textural Profile Analysis

The physicochemical characteristics of the optimized polyamide 6,10 monolithic matrices were investigated using textural profile analysis. The specific parameters determined include the matrix resilience (MR), matrix hardness (MH), deformation energy (DE) and the Brinell Hardness Number (BHN) using a calibrated Texture Analyzer (TA.XTplus, Stable Micro Systems, Surrey, England). These physicochemical parameters are defined in Chapters Two and Three of this dissertation. In order to determine these parameters, the textural settings and method described in Section 2.2.4 of Chapter Two were used. Typical force-time (for matrix resilience) and force-distance (for matrix hardness, deformation energy and the Brinell Hardness Number) profiles employed for the calculation of the physicochemical parameters are shown in Figures 2.2 and 3.3. The details of the calculations are explained in Chapters Two (Section 2.2.4) and Three (Section 3.2.4). All determinations were done in duplicate.

5.2.3. Determination of the Melting Point with Differential Scanning Calorimetry

The thermal properties of the optimized polyamide 6,10 variants (about 3mg of the powdered form of each) were analyzed using differential scanning calorimetry. The DSC

curves were recorded on a Perkin-Elmer Pyris-1 differential scanning calorimeter (Perkin Elmer, Boston, MA). Samples (10mg) were placed in crimped aluminium pans and heated from 25°C to 400°C at a rate of 10°C per minute under an inert nitrogen (purge gas) atmosphere.

5.2.4. Assessment of Semi-Crystallinity by X-ray Powder Diffractometry

Powder X-ray diffraction patterns of the powdered form of the optimized polyamide 6,10 variants were examined using the Bruker D8 Advance Diffractometer (Bruker, Karlsruhe, Germany). About 300mg of the sample was placed in the aluminium holder and subjected to the test. The X-ray diffractometer machine was operated at a generator voltage of 40kV, current of 30mA, scanning speed of 2 degrees per minute, step width 0.025 degrees, divergence slit 2mm, anti-scatter slit 2mm and detector slit of 0.2mm.

5.2.5. Scanning Electron Microscopy

This was utilized to identify and characterize the outer surface morphology of the three optimized polyamide 6,10 variants. This was achieved using the photomicrographs generated. Samples (10mmx10mm) were sputter-coated with gold-palladium (to minimize the absorbent or hydrophilic nature of the polyamides) and viewed under a JSM-840 Scanning Electron Microscope (JEOL 840, Tokyo, Japan) at a voltage of 20keV and a magnification of 1000x.

5.2.6. Fourier Transform Infrared Spectrophotometry

This was carried out in agreement with the method described in Chapter Two (Section 2.2.5) to establish the exact chemical structural backbone of the optimized polyamide 6,10 samples.

5.2.7. Molecular Mass Determination using Mass Spectrometry

The mass spectrum that generated the molar mass of the optimized polyamide 6,10 variants was recorded on the VG70 SEQ spectrophotometer (Micromass, UK) under high and low resolutions using powdered forms of the samples. The instrumental settings employed for the measurement include: ionization EI, Resolution 7500, Mass range 3.00amu (8\kv), Scan rate 5secs/decade (external). Approximately 2mg of the sample dissolved in about 2mL of meta-nitrobenzylalcohol was utilized in the study.

5.2.8. Water Uptake and Swelling Analysis

Water uptake and swelling evaluations for the three optimized polyamide 6,10 monolithic matrix formulations were studied under exactly the same conditions as described for the dissolution test in Chapter Three (Section 3.2.6.2).

The water uptake analysis was conducted in duplicate. The monolithic formulations were removed from the dissolution medium at the predetermined time intervals, lightly patted using lint-free tissue paper to remove excess liquid and weighed. Equation 5.1 expressed below was used to calculate the percentage weight gained at each time point.

$$\text{Quantity of Water Absorbed (g)} = \text{Wet Weight} - \text{Dry Weight} \quad (\text{Equation 5.1})$$

The matrix swelling analysis was conducted in duplicate. The dried and wet matrices can be described to have a cylindrical geometry. Therefore, the volumetric swelling is measured in place of the axial. Consequently, the, swollen volumetric dimensions for each formulation was measured using Equation 5.2, which is an expression of the formula used in calculating the volume of a cylinder.

$$\text{Volume} = \pi r^2 h \quad (\text{Equation 5.2})$$

where volume =volume of the cylinder (the monolithic matrix systems are likened to a cylinder), $\pi =3.143$, r =radius of the cylinder calculated as half of its diameter and h = height of the cylinder. The dry as well as wet (swollen) radii and heights of the matrices (discs) were measured using the manually operated Vernier caliper (25 X 0.01mm capacity, Germany).

After calculating the experimental changes in volume, the percentage volumetric swelling was computed using Equation 5.3.

$$\text{Volumetric Swelling (\%)} = \frac{\text{Swollen Thickness} - \text{OriginalThickness}}{\text{OriginalThickness}} \times 100 \quad (\text{Equation 5.3})$$

In addition, the relationship between the swelling as well as the water uptake characteristics of the matrix formulation and the total matrix thickness left on hydration was investigated through textural analysis of the dry as well as the hydrated matrices. The same procedural standards specified for the water uptake and swelling analyses were followed. The deformation energy (DE) described as the total work of probe penetration into the entire matrix was employed for this evaluation.

5.2.9. Conductivity Evaluation

Electrolyte conductivity evaluation was performed on the three optimized polyamide 6,10 monolithic matrices in duplicate. The methodology described for this experiment in Chapter Three (Section 3.2.8) was also employed in this case.

5.2.10. Dissolution and Matrix Erosion Analyses

Both experiments were performed on the optimized systems in accordance with the procedural stipulations described in Chapter Three (Section 3.2.7).

5.3. RESULTS AND DISCUSSION

5.3.1. Determination of the Physicomechanical Characteristic by Textural Profile

Analysis

The values of the physicomechanical parameters for both variants, which are a function of the matrix strength the dry matrices, are presented in Table 5.1. These revealed the differences between the physicomechanical strength of the optimized polyamide 6,10 matrices and a direct influence on drug release from the optimized polyamide 6, 10 monolithic matrix formulations (slow, controlled and controlled release formulations) with an increase in the magnitude of each physicomechanical parameter resulting in a decreased rate of drug release (Figure 3.11 and Table 5.1).

Table 5.1: Numerical values of the physicomechanical parameters that characterize the matrix strength and integrity of the optimized polyamide 6,10 matrices

Physicomechanical Parameters	Numerical values			Units
	“SR” ^e	“IR” ^e	“CR” ^e	
MR ^a	64.00	44.00	42.00	%
MH ^b	71.11	40.30	36.60	N/mm
DE ^c	0.05	0.03	0.02	Joule
BHN ^d	20.50	17.88	14.45	N/mm ²

^a Matrix Resilience; ^b Matrix Hardness; ^c Deformation Energy; ^d Brinell Hardness Number; ^e “SR”, “IR” and “CR” are the optimized monolithic matrix formulations namely the slow, intermediate and controlled release formulations respectively

5.3.2. Melting Temperature Determination using Differential Scanning Calorimetry

This technique was employed to characterize the thermal properties of the optimized polyamide 6,10 variants. The melting temperature (T_m) values were obtained from the thermograms of the three optimized monolithic formulations and the values enlisted in Table 5.2. Significant differences in the values of the melting temperatures were observed and this may be attributed to the modification of the synthesis process as the composition (based on the monomers, volume ratio and solvent phase modifiers) of each reaction vessel varied for each optimized sample.

Table 5.2: Numerical values of the melting temperature of the optimized polyamide 6,10 variants

Optimized Polyamide 6,10 Variants	Melting Temperature (°C)
“SR” ^a	214.00
“IR” ^a	204.00
“CR” ^a	182.00

^a “SR”, “IR” and “CR” are the optimized monolithic matrix formulations demonstrating slow, intermediate and controlled release respectively

The influence of the matrix physicochemical strength on the thermal characteristics is obvious (Tables 5.1 and 5.2) as an increase in matrix physicochemical strength resulted in an increase in the melting temperature. Also, an increase in melting temperature resulted in a decrease in the amount of drug released (i.e. a slower rate of drug release). Therefore, an increase or decrease in melting temperature may be directly related to an increase or decrease in matrix physicochemical strength based on this finding. In other words, a strong matrix (in terms of physicochemical strength) displayed a higher melting temperature as well as prolonged drug release behaviour. The

observed differences in the optimized polyamide 6,10 samples may be attributed to the difference in the intensity of the intramolecular hydrogen bonds (Figure 1.1) (due to process modification) within the polyamide linear chain.

Furthermore, the samples exhibited a double melting endotherm (Figure 5.1), which is a common phenomenon in even-even polyamides (Cui *et al.*, 2004). Some obvious exothermic peaks were noticed in the thermograms, which may be as a result of the multiple melting behaviors of the aliphatic polyamides in the melt-crystallized state described by Cui *et al.* (2004). A typical DSC thermogram of an optimized polyamide 6,10 sample is illustrated in Figure 5.1.

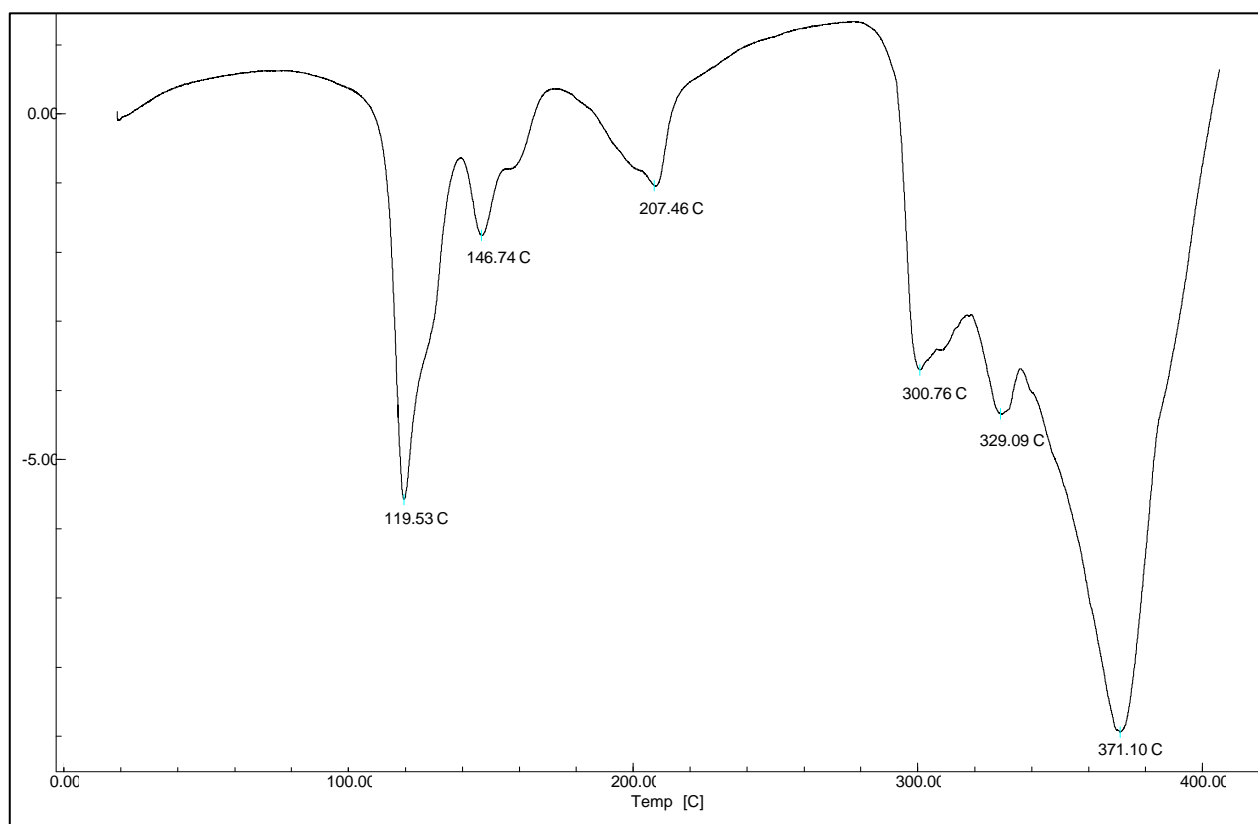


Figure 5.1: Typical DSC thermogram of an optimized polyamide 6,10 variant showing the melting temperature, double melting endotherm and exothermic peaks.

5.3.3. Elucidation of the Semi-Crystallinity of the Optimized Polyamide 6,10 Matrices by X-ray Powder Diffractometry

The diffractograms presented in Figure 5.2a, b and c display the X-ray diffraction patterns of the optimized polyamide 6,10 variants, namely, “SR”, “IR” and “CR” respectively. The prominent, sharp, high intensity as well as the blunt, low intensity peaks show that the samples contain both crystalline and amorphous segments (i.e. the semi-crystalline nature of polyamides) respectively. From the diffractograms, it was observed that the ratio of the amorphous domains to that of the crystalline domains varied from one optimized variant to the other (Figure 5.2). This variation may be responsible for the differences exhibited in the drug release characteristics of the optimized polyamide 6,10 monolithic matrix formulations.

The crystalline domain of the “SR” was the most, “IR” was less and “CR” was the least while the converse was observed for the amorphous portions (Figure 5.2 a, b and c). Therefore, an increase in the crystalline portion of the polyamide 6,10 reduced the rate of drug release and vice versa.

Based on the peak positions and intensities, a “search-match routine” analysis was performed on the respective diffractograms obtained. This analysis revealed that each optimized sample is composed of carbon (C), hydrogen (H), nitrogen (N) and oxygen (O) atoms, which correspond to the established chemical backbone structure of polyamide 6,10 (Figure. 2.1).

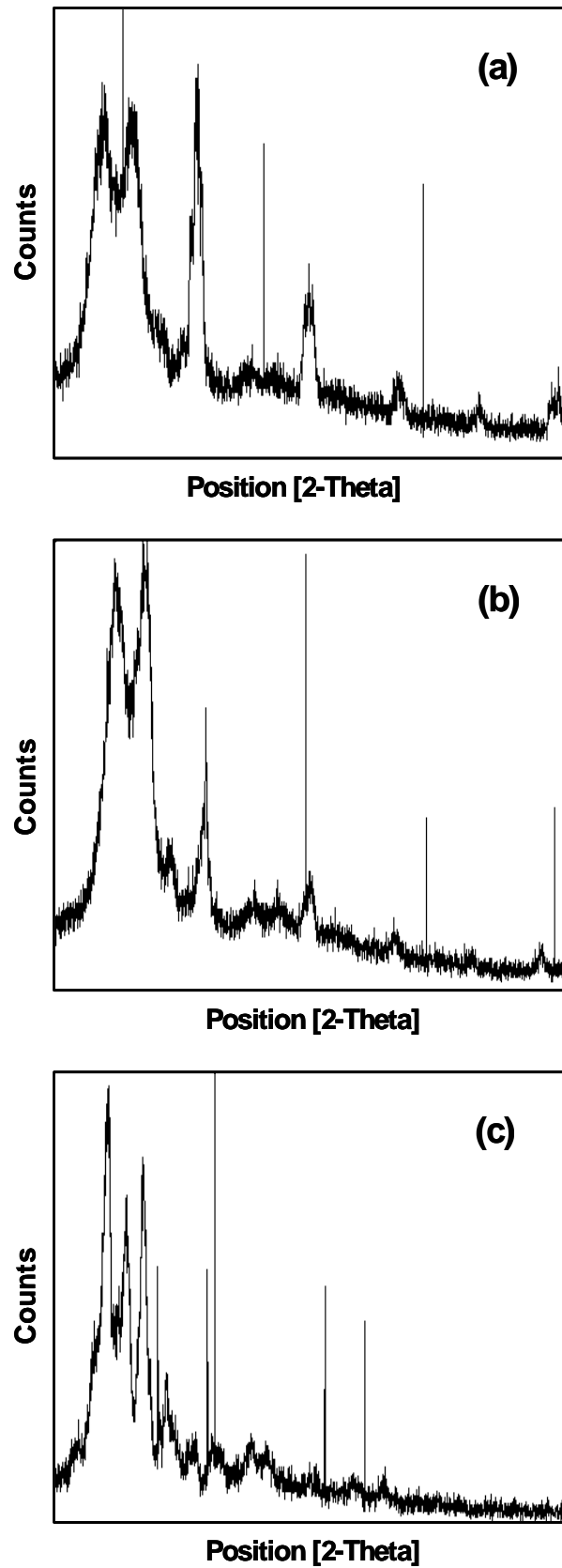


Figure 5.2: X-ray diffraction patterns of the (a) slow (b) intermediate and (c) controlled release formulations.

5.3.4. Assessment of the Surface Morphology of the Optimized Polyamide 6,10 Variants

The surface geometries of the optimized polyamide 6,10 variants were examined to reveal the differences that exist (Figure 5.3). Analysis showed conspicuous differences in the surface morphologies of each optimized polyamide 6,10 variant confirming the efficiency of the full modification strategy (stoichiometry, volume ratios of solvents as well addition of solvent phase modifiers) employed in the synthesis of these three optimized polyamide 6,10 variants influenced their surface morphologies. This transformations played a critical role in establishing their exhibited physicochemical and physicomechanical characteristics. The surfaces of “SR”, “IR” and “CR” on examination were dissimilar in surface geometry, topography and porosity.

The surface topography polyamide 6,10 variant that demonstrated slow release (“SR”) was continuous, relatively closely packed and compact (Figure 5.3a). The pore sizes appeared to be very small, tending towards being almost invisible. The close packaging of polymeric chain domains possibly minimizes water infiltration as well as burst effects and this may be responsible for slow release rates observed (Figure 3.11). This feature may also be linked with the high physicomechanical strength and melting temperature demonstrated by this variant (Tables 5.1 and 5.2).

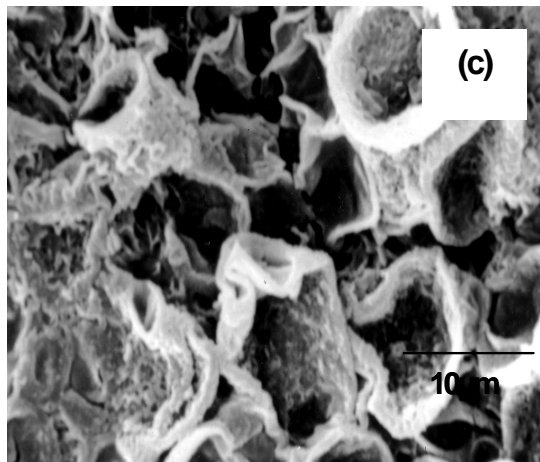
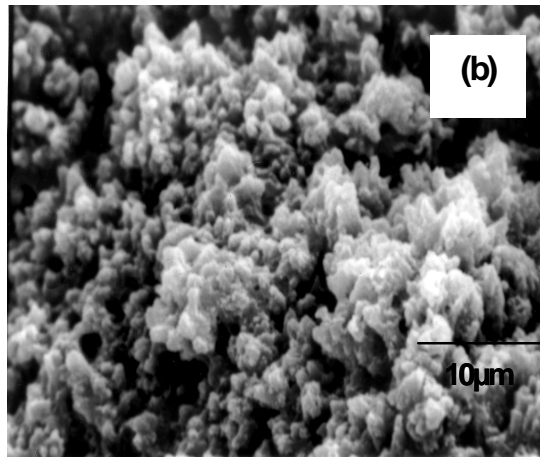
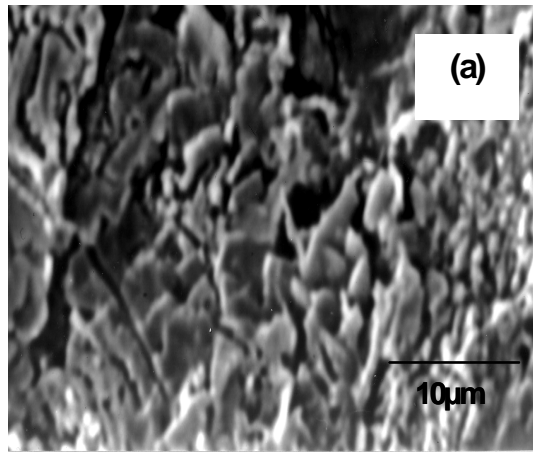


Figure 5.3: SEM micrographs of the (a) slow (b) intermediate and (c) controlled optimized polyamide 6,10 variants showing their surface morphological diversity (magnification $\times 1000$, voltage 20kV).

The “IR” variant on the other hand showed clustered geometry, which appears to be more porous than that of the “SR” variant (Figure 5.3b). This wobbly geometry would favour a more rapid influx of water molecules, as there are larger domains (pockets or pores) into which the water molecules would fit. Consequently, a quicker drug release rate is expected (Figure 3.11). These also may be related to its reduced mechanical strength and melting temperature which enhances the rate of polymeric matrix loosening and dissolution (Tables 5.1 and 5.2).

Lastly, the “CR” variant showed mushroom-like surface characteristics (Figure 5.3c), which has larger and most porous pores. This appearance can favour higher rates of water influx compared to the “SR” and “IR”. The drug release behaviour demonstrated by “CR” may be attributable its surface geometry (Figure 3.11). Also, a direct relationship between the physicomechanical, thermal and surface properties of “CR” can be proposed (Tables 5.1 and 5.2).

5.3.5. Fourier Transform Infrared Spectrophotometric Analysis

The FTIR spectra of the three optimized polyamide 6,10 variants (Figure 5.4) displayed peaks at the vibrational frequencies characteristic of the respective bonds present within the backbone structure of polyamide 6,10 (Figure 2.1). The numerical values for the salient bonds within the polyamide backbones are presented in Table 5.3.

A close relationship exists between the vibrational frequencies of the salient bonds of the optimized polyamide 6,10 variants. This shows that their basic chemical structural backbones are intact and closely related to the basic polyamide 6,10 structure. This shows that that the modification strategy employed in this study maintained the chemical

polyamide 6,10 structural backbone but influenced its physicochemical and physicomachanical characteristics. This may be associated with the influence of the modification on the intensity of the intramolecular hydrogen bond structure of the optimized variants (Figure 1.1), which is reflected by the values of the vibrational frequencies of each optimized polyamide 6,10 variant (Table 5.3). The FTIR spectra produced by the three samples were of comparable patterns and this also supports the findings. A typical FTIR spectrum of the optimized polyamide 6,10 variants is shown in Figure 5.4.

Table 5.3: Characteristic FTIR absorption frequencies of the selected and optimized polyamide 6,10 variants

Optimized Polyamide 6,10 Variants	C-H stretch	C-O	C=O	N-H	C-N	CH₂ wag	CH₂ rock
SR ^a	2978.00	1216.75	1711.11	3423.10	1334.77	1477.66	769.85
IR ^a	2897.11	1218.94	1710.55	3426.44	1336.47	1474.07	772.34
CR ^a	2923.13	1198.00	1712.22	3421.11	1337.77	1486.22	774.55

^a "SR", "IR" and "CR" are the slow, intermediate and controlled release optimized monolithic matrix formulations respectively

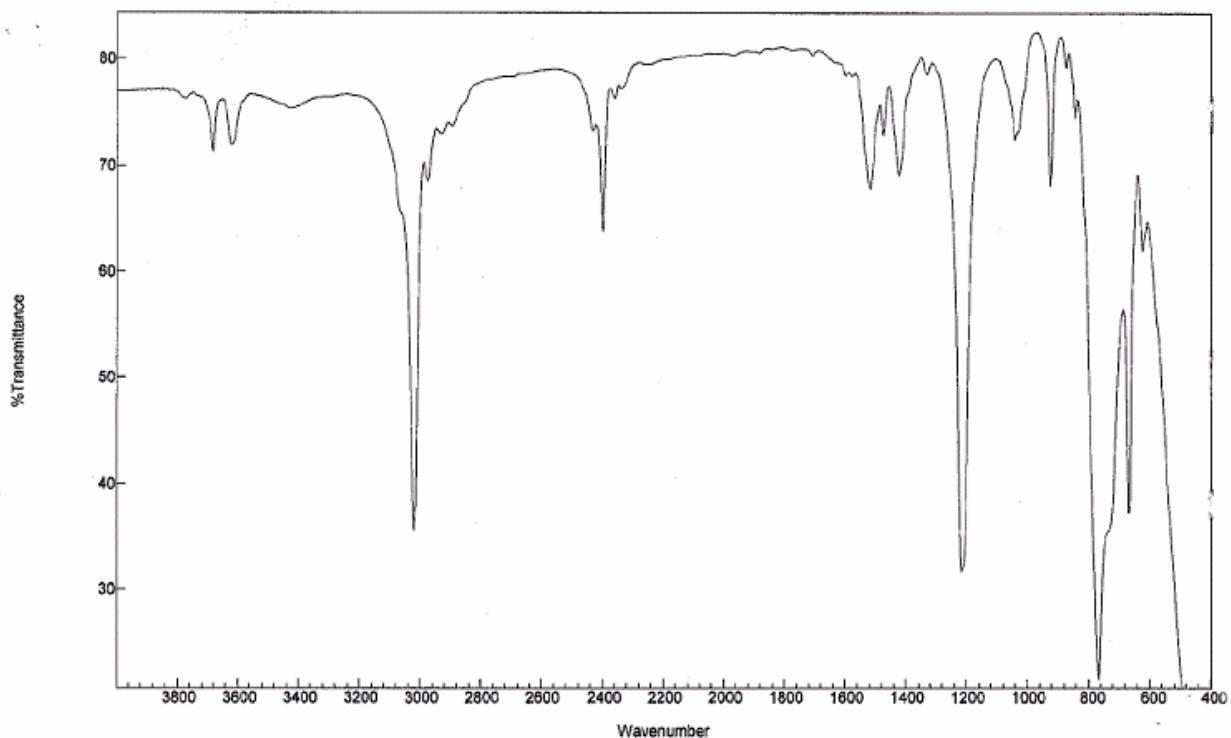


Figure 5.4: A Typical FTIR spectrum of an optimized polyamide 6,10 variant.

5.3.6. Determination of the Molecular Masses of the Optimized Polyamide 6,10 Variants

The mass spectrum of the three optimized polyamide 6,10 variants are outline as follows:

- (a) **Slow release variant** (“SR”): (EI) showed a strong peak in the positive mode at m/z **410.5** corresponding to $(M^+ + 1)$ for it.
- (b) **Intermediate release variant** (“IR”): (EI) showed a strong peak in the neutral mode at m/z **345.2** corresponding to (M^+) for it.
- (c) **Controlled release variant** (“CR”): (EI) showed a strong peak in the positive mode at m/z **307.2** corresponding to $(M^+ + 1)$ for it.

In other words, the stated results means that the optimized polyamide 6,10 variants had molecular masses (M_m) of **410.5g/mol, 345.2g/mol and 307.2g/mol** for “SR”, “IR” and

“CR” respectively. This showed that the modification strategy employed in this study had visible influence on the molecular mass of the respective optimized polyamide variants. An increase in molecular mass reduced the drug release velocity and vice-versa. In other words, “SR” demonstrating the slowest release rate (Figure 3.11) had the highest molecular mass ($M_m = 410.5$) while the converse ($M_m = 307.2$) was observed for “CR” that showed the quickest release rate (Figure 3.11). This implies that the molecular mass also has an influence on the rate of disentanglement as well as drug release of polyamide 6,10.

The outcome of this experiment may not necessarily imply that there is a chemical change within the backbone structure of the optimized polyamide 6,10 variants. The variations observed in the values of the molecular masses obtained may be due to the differences in the fragmentation pattern (into ions) of each optimized variants when bombarded with the electron beam of the mass spectrometer. This may be associated with the differences in the intensity of the intramolecular hydrogen bonding for each optimized variant.

5.3.7. Water Uptake and Swelling Analyses

5.3.7.1. Water Uptake

The monolithic matrix formulations prepared from the optimized polyamide 6,10 variant demonstrated the ability to absorb water measured in terms of the weight gained. The rates of absorption of water varied for each formulation and this can also be related to drug release profiles generated in Chapter Three (Figure 3.11). The graphical representations showing the quantity of water absorbed (water uptake), calculated using

equation 5.1, at particular time point for the three optimized variants at pH 7.4 is illustrated with Figure 5.5.

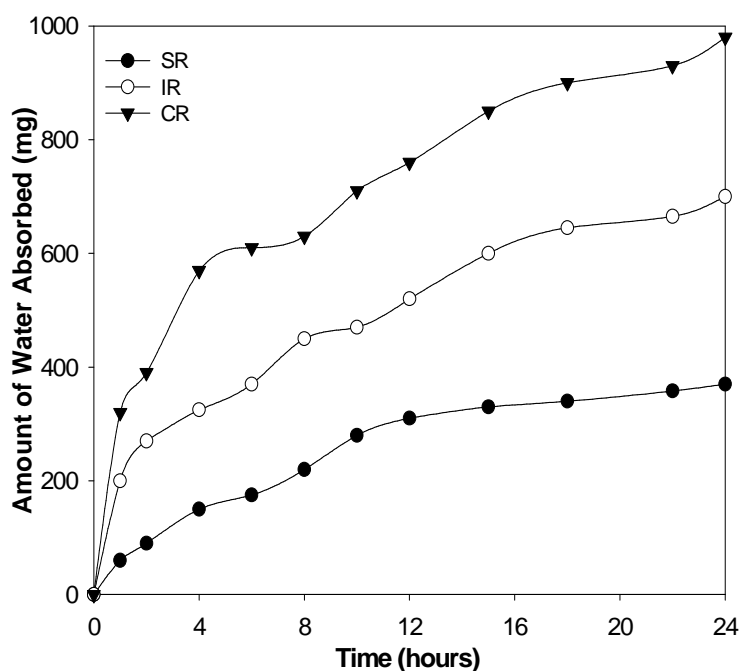


Figure 5.5: Water uptake of the optimized polyamide 6,10 monolithic matrices (N= 2 and standard deviation less than 5.11 in all cases).

Formulation “SR” absorbed the lowest amount of water and this may be responsible for its slow release rate when compared with formulations “IR” and “CR” (Figure 5.5). This shows that the rate polymeric wetting, disentanglement and drug diffusion is a function of the water uptake process.

5.3.7.2. Matrix Swelling

An initial increase (at the first hour) in volume of the monolithic matrices was observed for the three optimized formulations with formulation “CR” having the highest volume, formulation “SR” the lowest and formulation “IR” was in-between the two extremes (Figure 5.6). This may be associated with the capability of formulation “CR” to absorb

more aqueous when compared with the formulations “IR” and “SR”. A relatively constant increase in swelling front following the initial increase in matrix volume (swelling) on hydration (at the first hour) was observed for the three samples. In view of the fact that no significant increase in volumetric dimension (i.e. matrix swelling) was observed, it can be inferred that drug release from these matrices is controlled more by polymer disentanglement or relaxation followed by dissolution which facilitates drug diffusion out of the matrix. This pattern is contrary to that of most hydrophilic polymeric materials employed in rate controlled drug delivery as these have matrix swelling as a major phase of controlling release (Siepmann and Peppas, 2001b; Jamzad, 2005).

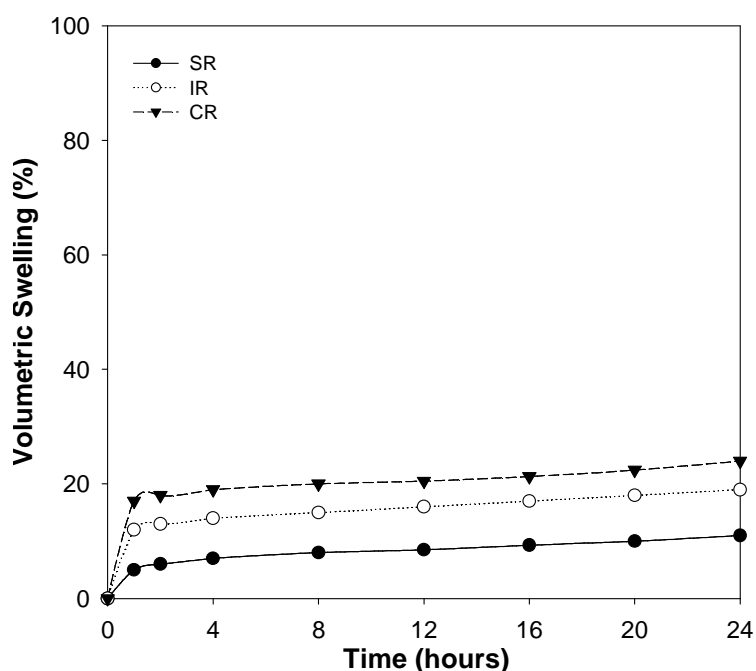


Figure 5.6: Volumetric swelling front movement for the optimized and selected polyamide 6,10 variants in buffer solutions of pH 7.4. (N= 2 and standard deviation less than 1.25 in all cases).

5.3.8. Conductivity Evaluation

This study was conducted in order to visualize the capability of the optimized polyamide 6,10 formulation to dissolve and generate polar ions in the dissolution media (Figure 3.8). Significant changes in conductivity values with time were observed for the three optimized polyamide 6,10 formulations (Figure 5.7) implying that the polymeric matrices can actually undergo dissolution to generate polar ions, which conduct current to generate the reading in microsiemens (μs).

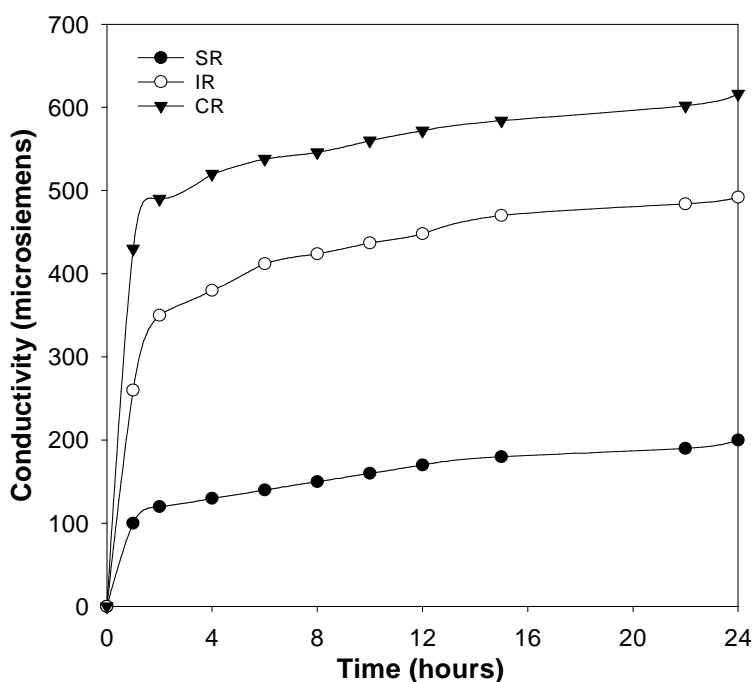


Figure 5.7: Change in conductivity values with time for the optimized polyamide 6,10 formulations (N= 2 and standard deviation less than 10.41 in all cases).

5.3.9. Dissolution and Matrix Erosion Analyses

Diverse dissolution profiles were produced for the optimized polyamide 6,10 formulation. This reflected the effect of the physicochemical and physicomechanical characteristics

influenced by method of synthesis (i.e. interfacial polymerization) on drug release characteristics (Figure 3.11).

Matrix erosion analysis for each optimized polyamide 6,10 matrix formulation was computed as percentage weight loss. Profiles for each formulation were related to the drug release performances (Figure 5.8).

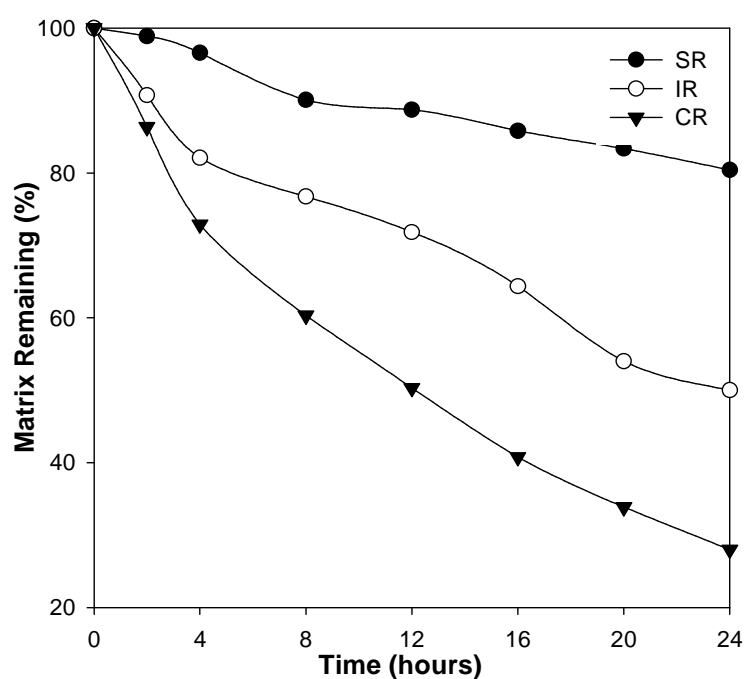


Figure 5.8: Matrix erosion analysis for the optimized polyamide 6,10 matrix formulations. (N= 2 and standard deviation less than 4.42 in all cases).

5.4. CONCLUDING STATEMENTS

The efficiency of modification strategy as well as statistical optimization of data in achieving desirable drug release characteristics has been established by this Chapter. The optimized polyamide 6,10 variants (i.e. “SR”, “IR” and “CR”) produced in this study based on the modification of the process of interfacial polymerization and statistical optimization have been successfully characterized based on their physicochemical and

physicomechanical properties. A relationship between the physical properties (i.e. physicochemical and physicomechanical) and drug release behaviour of the optimized polyamide 6,10 variants was observed.